



Molecular docking, 3D-QSAR studies of indole hydrazone as *Staphylococcus aureus* pyruvate kinase inhibitor

Srilata Ballu, Ramesh Itteboina, Sree Kanth Sivan, Vijjulatha Manga*

Molecular Modeling and Medicinal Chemistry Group, Department of Chemistry, University College of Science, Osmania University, Hyderabad – 07, India

Received: 10-09-2014 / Revised: 27-09-2014 / Accepted: 28-09-2014

ABSTRACT

Staphylococcus aureus is a bacterium that is a common cause of skin infection, respiratory disease and food poisoning. Pyruvate kinase is an enzyme involved in glycolysis. Inhibition of pyruvate kinase initiates reverse sequence of glycolysis that is lethal for bacterium. Docking and 3D quantitative structure activity relationship (3D-QSAR) studies were performed on 46 Indole hydrazone derivatives reported as inhibitors of Pyruvate kinase. Ligands were built and docked into protein active site using GLIDE 5.6. The docked poses were analyzed and the best docked poses were selected for further 3D-QSAR analysis using comparative molecular field analysis (CoMFA) and comparative molecular similarity indices analysis (CoMSIA) methodology. QSAR models were generated using 35 molecules in the training set. Developed models showed good statistical reliability which is evident from r^2_{ncv} and r^2_{loo} values. The predictive ability of these models was determined using a test set of 11 molecules that gave acceptable predictive correlation (r^2_{Pred}) values. CoMFA models provide the most significant correlation of steric and electrostatic fields with biological activities. CoMSIA model provides a correlation of steric, electrostatic, acceptor, donor and hydrophobic fields with biological activities. The information rendered 3D QSAR model initiated us to optimize the lead and design new potential inhibitors.

Key Words: CoMFA (Comparative molecular field analysis), CoMSIA (Comparative molecular similarity indices analysis), PLS (partial least square) analysis, PK (pyruvate kinase), MRSA (Methicillin-resistant *Staphylococcus aureus*)



INTRODUCTION

Staphylococcus aureus is a gram positive coccus bacterium that is a member of the Firmicutes, and is commonly found in the human respiratory tract and on the skin. *S. aureus* is a common cause of skin infections, respiratory disease and food poisoning. Disease-associated strains often promote infections by producing potent protein toxins, and expressing cell-surface proteins that bind to antibodies and inactivate them. The emergence of antibiotic-resistant forms of pathogenic *S. aureus* e.g. methicillin-resistant *Staphylococcus aureus* (MRSA) and vancomycin-resistant I (VRSA) have become worldwide problem in clinical medicine. Pyruvate kinase (PK) is one of the most highly connected 'hub proteins' in MRSA. [1] PK is critical for bacterial survival which makes it a potential target for development of novel antibiotics and the high degree of connectivity implies it should be very sensitive to mutations and

thus less able to develop resistance. Pyruvate kinase [2] is an enzyme involved in glycolysis. It catalyses the transfer of a phosphate group from phosphoenolpyruvate to ADP, yielding one molecule of pyruvate and one molecule of ATP. PK has human homologous enzymes that has unique peptide sequence insertion and deletion differences from the bacterial enzymes, this produces druggable lipophylic pockets on the bacterial enzyme that are absent on the human forms. One of these pockets was probed in an in silico screening effort [3]. Computational drug design approaches are vastly employed in development and optimization of inhibitors. A detailed study of molecular interactions of pyruvate kinase inhibitors with the protein will help in design of novel molecules for better antibacterial activity. Our main objective was to obtain structural requirements for pyruvate kinase inhibitors and design novel molecules. In present article we report receptor based 3D-QSAR [4-7]

*Corresponding Author Address: Dr. Vijjulatha Manga, Molecular Modeling and Medicinal Chemistry Group, Department of Chemistry, University College of Science, Osmania University, Hyderabad – 07, India; E-mail: vijjulathamanga@gmail.com

studies using CoMFA [8, 9] and CoMSIA [10] methodologies on indole hydrazone derivatives [11]. Partial least square (PLS) [12] based statistical analysis was carried out on 46 molecules to identify the correlation. The contour maps generated enabled us to explain the observed variation in activity and guided us to design new molecules.

METHODOLOGY

The crystal structure of *staphylococcus aureus* pyruvate kinase (pdb id: 3TOT) [13] was downloaded from the protein databank. GLIDE 5.6 [14] was used for molecular docking. The protein was prepared using protein preparation module applying the default parameters, a grid was generated around the active site of the pyruvate kinase with receptor van der Waals scaling for the nonpolar atoms as 0.9 [15]. A set of 46 known pyruvate kinase inhibitors were selected from literature [11]. These were built using maestro build panel and prepared by Lig prep application in Schrödinger 2010 suite. The molecular docking of the 46 molecules into the generated grid was performed by using the extra – precision (XP) docking mode [16]. The crystal structure ligand was also docked and its root mean square deviation (RMSD) was calculated to validate the docking process. The analysis of dock poses of all the molecules showed similar hydrogen bond interaction with the active site residue. The best dock pose for each molecule was chosen for CoMFA and CoMSIA analysis without further alignment that is super imposition of ligands based on the common substructure for a set of molecule was not done, docked based alignment is shown in figure 2. The molecules were imported into SYBYLX1.2 [17] molecular modeling program package, Gasteiger-Huckel charges [18] were assigned. The standard Tripos force fields were employed for the CoMFA and CoMSIA analyses. A 3D cubic lattice of dimension 4 Å in each direction with each lattice intersection of regularly spaced grid of 2.0Å was created. The steric and electrostatic parameters were calculated in case of the CoMFA fields while hydrophobic, acceptor and donor parameters in addition to steric and electrostatic were calculated in case of the CoMSIA fields at each lattice. The SP³ carbon was used as a probe atom to generate steric (Lennard Jones potential) field energies and a charge of +1 to generated electrostatic (Columbic potential) field energies. A distance dependent dielectric constant of 1.00 was used. The steric and electrostatic contributions were cut off at 30 k cal mol⁻¹. A partial least squares (PLS) regression was used to generate a linear relationship that correlates changes in the computed fields with changes in the

corresponding experimental values of biological activity (pKi) for the data set of ligands. The data set was divided into training set consisting of 35 molecules and test set of 11 molecules. Biological activity values of ligands were used as dependent variables in a PLS statistical analysis. The column filtering value (s) was set to 2.0 K cal mol⁻¹ to improve the signal-to-noise ratio by omitting those Lattice points whose energy variation were below this threshold. Cross-validation was performed by the leave-one-out (LOO) procedure to determine the optimum number of components (ONC) and the coefficient r^2_{loo} . Optimum number of components obtained is then used to derive the final QSAR model using all of the training set compounds with non-cross validation and to obtain the conventional regression coefficient (r^2). To validate the CoMFA and CoMSIA derived models, the predictive ability for the test set compounds (expressed as r^2_{pred}) was determined by using the following equation.

$$r^2_{\text{pred}} = (\text{SD-PRESS})/\text{SD}$$

SD is the sum of the squared deviation between the biological activities of the test set molecules and the mean activity of the training set compounds. PRESS is the sum of the squared of the deviation between the observed and the predicted activities of the test set compounds. Since the statistical parameters were found to be the best for the model from the LOO method, it was employed for further prediction of the designed molecules. The designed molecules were also constructed, minimized and docked into the protein active site same as mentioned above.

RESULTS AND DISCUSSION

Evaluation of accuracy of docking process is determined by measuring how closely the lowest energy pose (binding conformation) predicted by the object scoring function (Glide score), resembles an experimental binding mode as determined by X-ray crystallography. In the present study extra precision glide docking procedure was validated by removing compound 22 from the binding site and redocking it into the binding site of pyruvate kinase. We found a very good agreement between the localization of the inhibitor upon docking and from the crystal structure. The root mean square deviation between the predicted conformation and the observed X-ray crystallographic conformation of compound 22 equaled 0.267 Å (figure 3), a value that suggests the reliability of Glide docking in reproducing the experimentally observed binding mode for pyruvate kinase inhibitor and the parameter set for the docking is reasonable to reproduce the X-ray structure. The 3D-QSAR CoMFA and CoMSIA analysis were carried out

using indole hydrazone derivatives reported as Pyruvate kinase inhibitors. Molecules having inhibitory activity against pyruvate kinase enzyme with precise IC_{50} values were selected. A total of 46 molecules were used for derivation of model, these were divided into training set of 35 molecules and test set of 11. Keeping in view that the activity range is with a minimum of 2.8 log unit differences in both the sets.

The CoMFA and CoMSIA statistical analysis is summarized in table 1, Statistical data shows q^2_{loo} 0.606 for CoMFA 0.548 for the CoMSIA models, r^2_{nov} of 0.965 for CoMFA and 0.911 for CoMSIA which indicates a good internal predictive ability of the models. To test the predictive ability of the models, a test set of 11 molecules excluded from the model derivation was used. The predictive correlation coefficient r^2_{pred} of 0.65 for CoMFA and 0.66 for the CoMSIA models indicate good external predictive ability of the models. The experimental and predicted activity from CoMFA and CoMSIA model is given in table 2. Scatter plot of experimental vs predicted pIC_{50} values is represented in figure 4.

To visualize the information content of the derived 3D-QSAR model, CoMFA and CoMSIA contour maps were generated. Contour plots are the representations of the lattice points and the difference in the molecular field values at lattice points is strongly connected with difference in the receptor binding affinity. Molecular fields define the favorable or unfavorable interaction energies of docked molecules with a probe atom traversing across the lattice grid points surrounding the molecules. The 3D colored plots suggest the modification required to design new molecules. The contour maps of CoMFA denote the region in the space where the docked molecules would favorably or unfavorably interact with the receptor while the CoMSIA contour maps denote those areas within the specified region where the presence of a group with a particular physicochemical activity binds to the receptor. The CoMFA/CoMSIA results were graphically interpreted by field contribution maps using the "STDEV*COEFF" field type. Figure 5 (a, b) shows the contour maps derived from the CoMFA PLS model. The most potent analogue, compound 10, was embedded in the map (a), while least active compound 24 was embedded in the map (b) to demonstrate its affinity for the steric and electrostatic regions of inhibitors. The areas of yellow indicates region of steric hindrance to activity, while green areas indicate a steric contribution to potency. The blue regions indicate positive electrostatic charge potential associated

with increased activity, while red region show negative charge potential.

Substitutions at 3rd position of indole ring orient towards disfavored yellow region, indicates substitution at this position with bulky group leads to decrease in the activity. Bromo group is oriented towards sterically favored region, substitution at this position with bulky groups will increase the activity. The carbonyl group is oriented toward blue region indicating unfavored negative electrostatic potentials. All these explain the highest activity of the compound. The presence of a bulkier group on phenyl ring should increase the activity. This is evident from compounds 43, 44, 45 and 46 which are having a naphthyl ring instead of phenyl.

Figure 6, 7, 8 shows the contour maps derived from the CoMSIA PLS model. The most potent analogue, compound 10, was embedded in the map (a, c), while least active compound 24 was embedded in the map (b, d) to demonstrate its affinity for the steric, electrostatic, hydrophobic, H-bond acceptor and H-bond donor regions of inhibitors. The steric map is similar to the CoMFA steric map showing favored and disfavored regions. Absence of steric group at benzoyl ring in compound 24 shows lower activity; where as in compound 10, bromide substitution on benzoyl ring increased the activity.

The electrostatic contour maps show a red region near the nitrogen and 3rd position of indole ring indicating a negative electrostatic potential, should increase the potency as seen in the case of compound 10. The blue regions near the 4th, 5th and 6th position of indole indicates a region with positive electrostatic potential. The hydrophobic contour show a favored yellow region near the 2nd position of benzoyl ring and a hydrophilic white region covering whole molecule except hydrazone moiety and -CO, -OH groups of benzoyl ring. The magenta and red contours represent favorable and unfavorable H-bond acceptor groups respectively. The H-bond acceptor contour maps show the favored region for hydrogen bond acceptor groups near the -NH group of indole ring and a disfavored region for hydrogen bond acceptor near the -CO and -OH group of benzoyl ring.

The cyan and purple contour represents favorable and disfavorable hydrogen bond donor groups respectively. The H-bond donor contour maps showed favored region for hydrogen bond donor groups near -OH of benzoyl ring. The detailed contour map analysis of both CoMFA and CoMSIA models empowered us to identify structural requirements for the inhibitory activity.

The molecules were modified further to improve the inhibition activity toward Pyruvate kinase. Compound 10 having best activity was chosen as a reference structure to design new molecules (Figure 10) to obtain a greater number of new potent molecules. The newly designed molecules were docked into the protein active site. Dock poses were used to predict the activity by applying the 3D-QSAR model. The new molecules showed better dock score and predicted activity (Table 3).

Newly designed compounds were analyzed for drug-likeness by assessing their physiochemical properties (Table 4) and by applying Lipinski's rule of five. The Lipinski's rule for drug like molecules states that the molecule should have molecular weight <650 Daltons, H-bond donors <5, H-bond acceptors <10, and a log P of <5. For the designed molecules, the partition coefficient (QPlogPo/w) and water solubility (QPlogS) are critical for estimating the absorption and distribution of drugs within the body, which ranged between 4.148-6,219 and 5.914-8.461, respectively. Caco-2 cell permeability (QPPCaco), a model governing gut-blood barrier, ranged from 542.81 to 1354.462. MDCK cell permeability (QPPMDCK), a model that mimics the blood brain barrier, ranges from 1248.378 to 10000. Further, the predicted percentage human oral absorption for 5 molecules is 100%. All these pharmacokinetic parameters were found to be with in the acceptable range (table 4), out of five molecules, two molecules deviated from QPlogS due to CF₃ that reduced the solubility of designed molecule.

CONCLUSIONS

3D-QSAR is widely employed to develop new molecules that have an improved biological activity. CoMFA and CoMSIA methodologies were used to build models for Pyruvate kinase inhibitory activity of the Indole hydrazone derivatives. Based on the detailed contour map analysis, improvement in pyruvate kinase binding affinity can be achieved through conformationally restricted substitution at the benzoyl ring, maintaining the hydrogen bond donor character with less steric hindrance at these regions. The designed molecules based on these parameters showed better activity than the reference molecules, which indicates that the 3D-QSAR model generated has a good predictive ability and can be used to design new molecules with better activity.

ACKNOWLEDGMENTS

We greatly acknowledge Tripos Inc USA and Schrödinger LLC, New York for providing us the software. This research was made possible through grants from DST-SERB (SB/EMEQ-004/2013), CSIR (01/ (2436)/10/EMR-II), and UGC (42-233/2013(SR)), New Delhi, India. The authors SB and RI would like to acknowledge financial support from UGC for research fellowship. We wish to express our gratitude to Department of Chemistry, Osmania University for providing facilities to carry out the research work.

TABLE 1: PLS RESULT SUMMARY

Statistical parameters	CoMFA	CoMSIA
Q_{lo}^2 ^a	0.606	0.548
Number of molecules in training set	35	35
Number of molecules in test set	11	11
ONC ^b	6	5
SEE ^c	0.133	0.210
r^2 ^d	0.965	0.911
F_{ratio} ^e	129.977	59.083
r_{pred}^2 ^f	0.65	0.66
Fraction of fields contributions		
Steric	67.4%	15.5%
Electrostatic	32.6%	25.8%
Hydrophobic	--	31.4%
Acceptor	--	17.5%
Donor	--	9.7%

a – Cross-validation correlation coefficient by leave one out method,

b – Optimum number of components

c – Standard error of estimate

d – Conventional correlation coefficient

e – Fisher test value

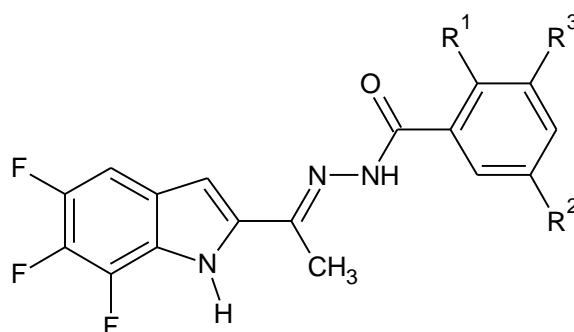
f – Cross-validation correlation coefficient on test set.

TABLE 2: EXPERIMENTAL pIC₅₀, PREDICTED pIC₅₀ AND GLIDE SCORES OF PYRUVATE KINASE INHIBITORS

Compound	Expt. pIC ₅₀	Pred. pIC ₅₀ CoMFA	Pred. pIC ₅₀ CoMSIA	Glide Score (kcal/mol)
1	7.070	6.834	6.724	-8.671
2	7.309	7.438	7.319	-8.327
3	7.283	7.247	7.268	-8.298
4	7.309	7.404	7.337	-8.284
5	7.366	7.357	7.279	-8.292
6 ^t	6.669	7.014	7.053	-8.177
7	7.619	7.509	7.603	-8.147
8 ^t	7.690	7.548	7.451	-8.581
9	7.619	7.641	7.426	-8.715
10	7.823	7.768	7.692	-8.698
11	6.782	6.827	6.689	-8.266
12	6.642	6.608	6.624	-7.651
13 ^t	6.835	6.904	6.576	-7.647
14 ^t	6.100	6.602	6.410	-7.683
15 ^t	7.769	6.482	6.471	-7.594
16	7.210	6.988	7.005	-8.062
17 ^t	6.838	7.030	6.969	-8.015
18 ^t	7.259	6.957	7.183	-7.962
19	6.419	6.210	6.025	-8.199
20 ^t	6.540	6.556	6.073	-8.208
21	6.649	6.645	6.631	-7.906
22	7.040	7.034	6.995	-7.771
23	6.643	6.613	6.780	-7.529
24	5.064	5.050	5.550	-8.215
25	5.882	6.097	5.735	-8.719
26	6.821	6.997	7.257	-8.769
27	6.739	6.815	6.913	-8.912
28	7.200	7.296	7.197	-9.000
29	6.600	6.625	6.594	-8.638
30	7.193	7.119	7.042	-7.623
31	7.130	7.075	7.041	-8.781
32	6.849	6.490	6.540	-8.637
33	6.316	6.647	6.483	-8.102
34 ^t	6.075	6.473	6.383	-8.692
35	6.063	6.122	6.320	-8.511
36	6.899	6.783	6.833	-8.832
37 ^t	6.345	6.005	6.115	-8.142
38	7.309	7.238	7.404	-8.298
39	6.774	6.774	6.696	-7.518
40	5.510	5.508	5.528	-7.860
41 ^t	6.336	6.020	5.971	-8.307
42	5.218	5.198	5.156	-8.334
43	7.376	7.227	7.147	-9.773
44	6.939	7.024	6.965	-8.049
45	7.102	7.103	7.255	-8.163
46	7.283	7.456	7.663	-9.341

t=Test set molecule

TABLE 3: GLIDE SCORE AND PREDICTED ACTIVITY OF NEWLY DESIGNED MOLECULES:



Compound	R ¹	R ²	R ³	Pred pIC ₅₀ CoMFA	Pred pIC ₅₀ CoMSIA	Glide Score (kcal/mol)
1	NH ₂	Br	H	7.336	7.321	-7.898
2	NH ₂	CH ₃	H	7.091	7.103	-8.509
3	NH ₂	Cl	H	7.076	7.112	-8.468
4	H	CF ₃	H	7.047	7.334	-8.719
5	H	CF ₃	CF ₃	7.010	7.650	-8.673

TABLE 4: ADME PROPERTIES OF NEWLY DESIGNED MOLECULE:

Compound ^a	QPlogPo/w ^b	QPlogS ^c	QPPCaco	QPPMDCK	%Human oral absorption
1	4.407	-6.190	542.802	3315.282	100
2	4.148	-5.914	542.177	1248.378	100
3	4.331	-6.076	542.734	3082.835	100
4	5.232	-7.016	1353.121	10000	100
5	6.219	-8.461	1354.462	10000	100

a. Newly designed molecules.

b. Predicted octanol/water partition coefficient log P (Acceptable range-2.0 to 6.5)

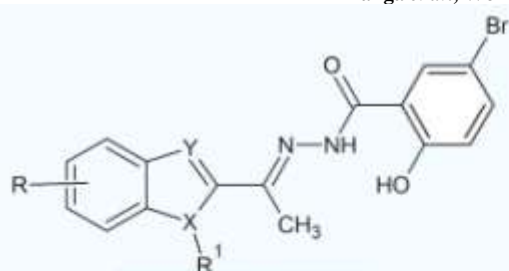
c. Predicted aqueous solubility's in mol/L (Acceptable range -6.5 to 0.5)

d. Predicted BBB permeability (Acceptable range-3 to 1.2)

e. Predicted Caco cell permeability in nm/s (Acceptable range :< 25 is poor and >500 is great)

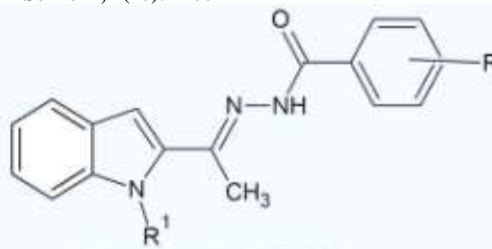
f. Predicted apparent MDCK cell permeability in nm/s (Acceptable range in nm/s (Acceptable range : < 25 is poor and >500 is great)

g. Percentage of human oral absorption (Acceptable range: <25 is poor and >80% is high).



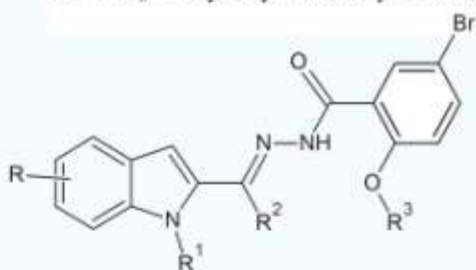
Compounds 1 -23

	R ¹	R	X	Y
1	H	H	N	C
2	H	5-flouro	N	C
3	H	5-chloro	N	C
4	H	5-bromo	N	C
5	H	5-iodo	N	C
6 ^t	H	5-hydroxy	N	C
7	H	6-bromo	N	C
8 ^t	H	5,6-diflouro	N	C
9	H	4,5-diflouro	N	C
10	H	4,5,6-triflouro	N	C
11	CH ₃	5-flouro	N	C
12	CH ₃	5-chloro	N	C
13 ^t	CH ₃	5-bromo	N	C
14 ^t	CH ₃	5-methoxy	N	C
15 ^t	CH ₃	6-bromo	N	C
16	CH ₃	5,6-flouro	N	C
17 ^t	CH ₃	4,5-flouro	N	C
18 ^t	CH ₃	4,5,6-flouro	N	C
19	CH ₃	H	N	C
20 ^t	H	H	C	S
21	H	H	N	S
22	H	H	N	NH
23	H	H	N	NCH ₃



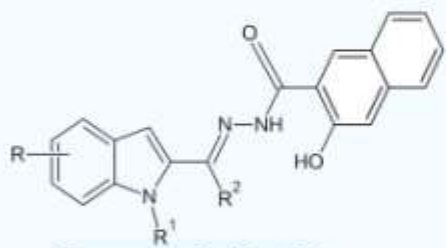
Compounds 24 - 34

	R ¹	R
24	H	2 ^t -hydroxy
25	H	2 ^t -hydroxy,4 ^t -bromo
26	H	2 ^t -hydroxy,5 ^t -iodo
27	H	2 ^t -methoxy,5 ^t -bromo
28	H	2 ^t -ethoxy,5 ^t -bromo
29	H	2 ^t -ethoxy methoxy-5 ^t -bromo
30	H	2 ^t -(prop-2yne-1-yloxy)-5 ^t -bromo
31	H	2 ^t -hydroxy-3 ^t ,5 ^t -dibromo
32	H	2 ^t -hydroxy-4 ^t -methoxy, 5 ^t -bromo
33	CH ₃	2 ^t -hydroxy-5 ^t -iodo
34 ^t	CH ₃	2 ^t -hydroxy-4 ^t -methoxy-5 ^t -bromo



Compounds 35 - 42

	R ¹	R ²	R3	R
35	H	H	H	H
36	H	C ₂ H ₅	H	H
37 ^t	H	H	CH ₃	H
38	H	C ₂ H ₅	H	5-bromo
39	CH ₃	C ₂ H ₅	H	5-bromo
40	CH ₃	H	H	H
41 ^t	CH ₃	C ₂ H ₅	H	H
42	CH ₃	Ph	H	H



Compounds 43 - 46

	R ¹	R ²	R
43	H	CH ₃	H
44	CH ₃	CH ₃	5-bromo
45	CH ₃	C ₂ H ₅	5-bromo
46	CH ₃	C ₂ H ₅	4,5,6-trifluoro

Figure 1: Structure of *s. aureus* pyruvate kinase inhibitors

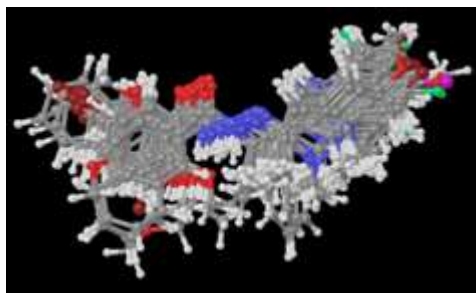


Figure 2: Docked base alignment of indole hydrazone derivatives.

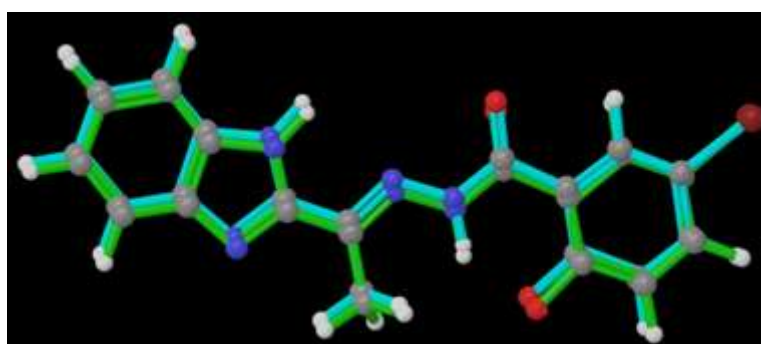


Figure 3: Superimposition of crystal structure pose (green) on docked pose (blue) of co-crystallized ligand. the rms deviation is 0.267Å

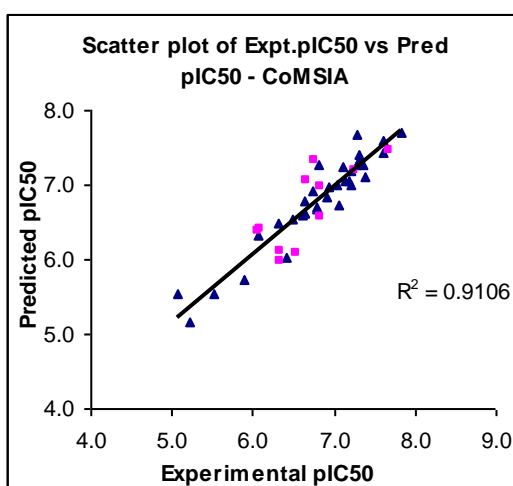
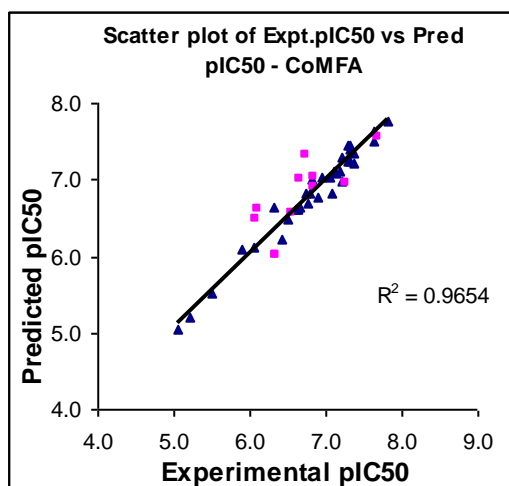
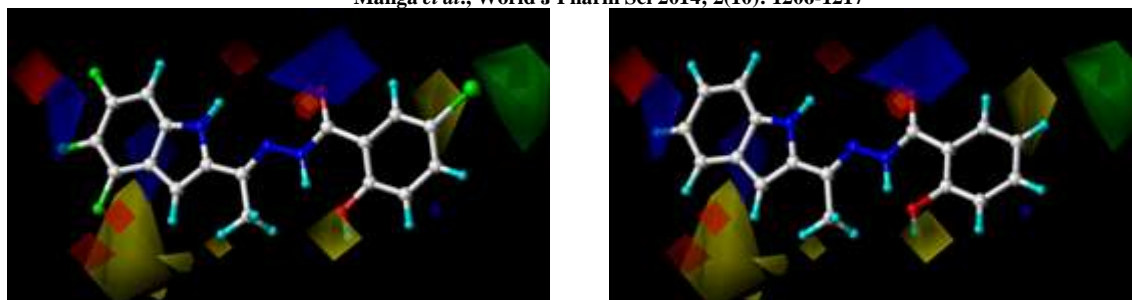


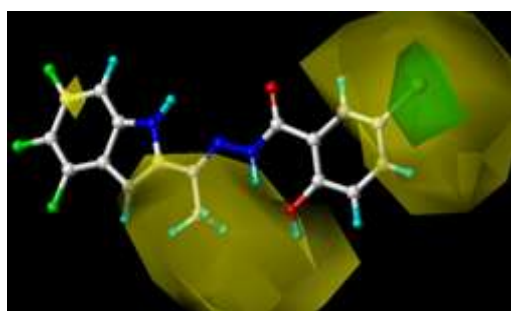
Figure 4: scatter plot of predicted vs experimental pIC₅₀ values (test set is represented as squares and training set represented as triangles)



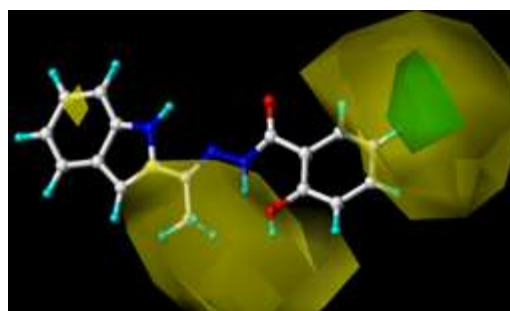
(a)

(b)

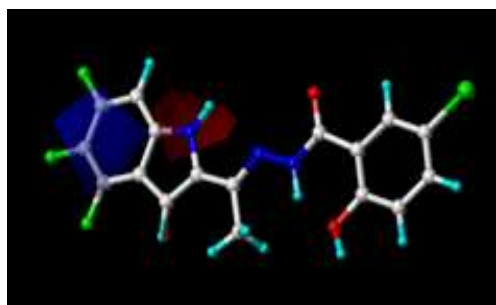
Figure 5: CoMFA steric standard deviation (s.d.* coefficient) contour maps illustrating steric and electrostatic features in combination with compound (a) 10 and (b) 24. green contours show favorable bulky group substitution at that point while yellow regions show unfavorable bulky group for activity. red contours indicate negative charge favoring activity. whereas blue contours indicate positive charge favoring activity.



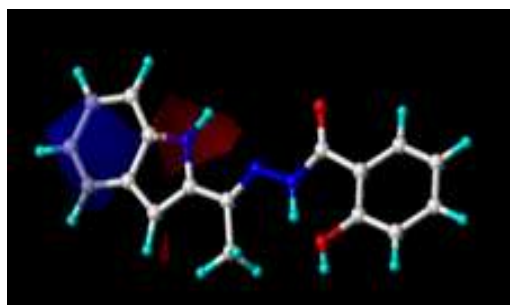
(a)



(b)



(c)



(d)

Figure 6: CoMSIA s.d.* coefficient contour maps illustrating steric and electrostatic features in combination with compound 10 and 24. (a,b) the green contour indicates a sterically favored region; yellow maps calls for a reduction of this potential to improve activity. (c, d) blue indicates a positive charge preferred region to improve activity; red indicates a negative charge preferred region to improve activity.

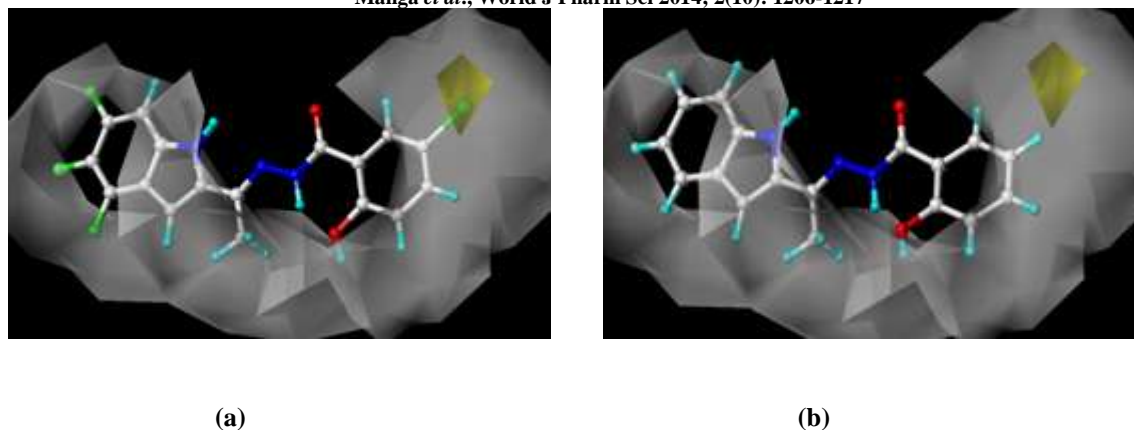


Figure 7: CoMSIA s.d.* coefficient contour maps illustrating hydrophobic features in combination with compound 10 and 24. (a, b) the yellow contour for hydrophobic favored region, white indicates the hydrophilic favored region.

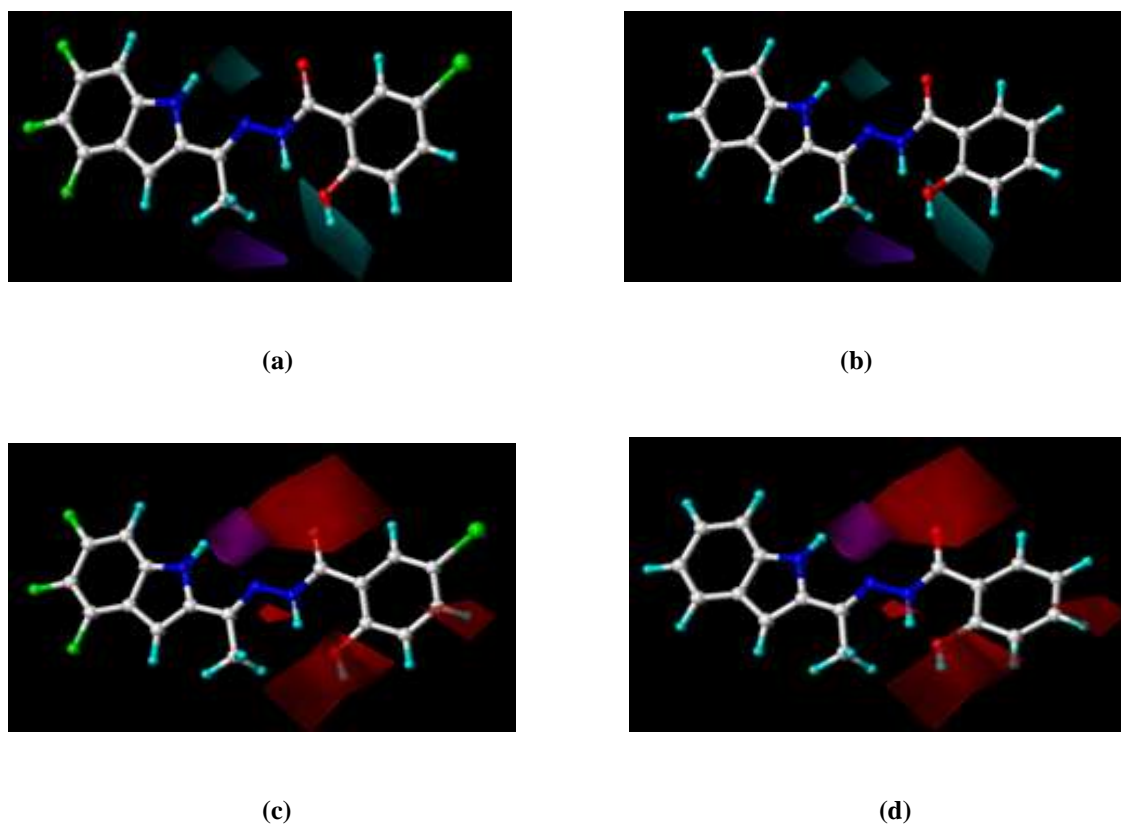


Figure 8: CoMSIA s.d.* coefficient contour maps illustrating acceptor and donor features in combination with compound 10 and 24. (a, b) the cyan contour for h-bond donor group increase activity, purple indicates the disfavored region. (c,d) the magenta contour for h-bond acceptor group increase activity, red indicates the disfavored region.

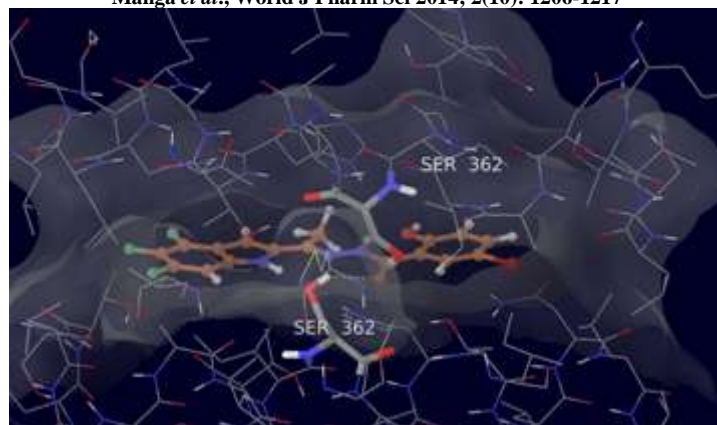


Figure 9: Docked pose of molecule 10 in the protein active site. showing the hydrogen bond interaction (yellow lines) with Ser 362.

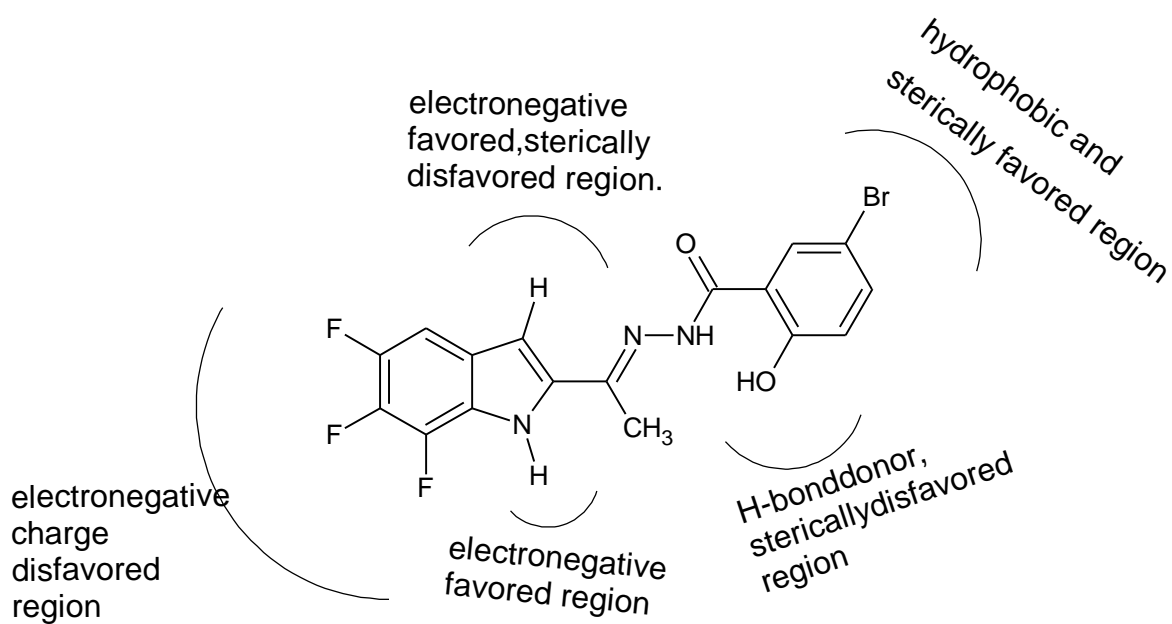


Figure 10: structure requirements for binding and inhibitory activity of indole hydrazone

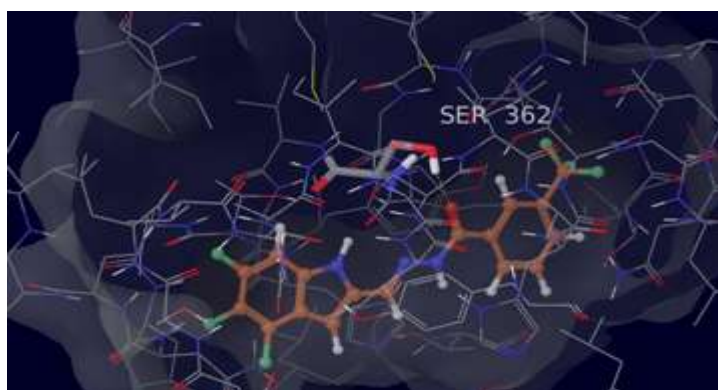


Figure 11: Docked pose of newly designed molecule 4 in the protein active site. showing the hydrogen bond interaction (yellow lines) with Ser 362.

REFERENCES

1. Cherkasov A *et al.* Mapping the Protein Interaction Network in Methicillin-Resistant *Staphylococcus aureus*. *J Proteome Res* 2011; 10: 1139-1150.
2. Nag SK *et al.* Discovery and optimization of a new class of pyruvate kinase inhibitors as potential therapeutics for the treatment of methicillin-resistant *Staphylococcus aureus* infections. *Bioorg Med Chem* 2014; 22: 1708-1725.
3. Axerio-Cilies P *et al.* Cheminformatics-Driven Discovery of Selective, Nanomolar Inhibitors for Staphylococcal Pyruvate Kinase. *ACS Chem Biol* 2012; 7: 350-359.
4. Caflisch A, Ehrhardt C. Structure-based combinatorial ligand design. In: *Structure based drug design*, Veerapandian P, Ed. Marcel Dekker, NY, **1997**; pp. 541- 558.
5. Cho SJ *et al.* Structure-Based Alignment and Comparative Molecular Field Analysis of Acetylcholinesterase Inhibitors. *J Med Chem* 1996; 39: 5064-5071.
6. Sippl W *et al.* Structure-based 3D QSAR and design of novel acetylcholinesterase inhibitors. *J Comput-Aided Mol Des* 2001; 15: 395-410.
7. Sippl W. Receptor-based 3D QSAR analysis of estrogen receptor ligands merging the accuracy of receptor-based alignments with the computational efficiency of ligand-based methods. *J Comput-Aided Mol Des* 2000; 14: 559-572.
8. Cramer RD *et al.* Comparative molecular field analysis (CoMFA). 1. Effect of shape on binding of steroids to carrier proteins. *J Am Chem Soc* 1988; 110: 5959-5967.
9. Cramer RD *et al.* Crossvalidation, bootstrapping, and partial least squares compared with multiple regression in conventional QSAR studies. *Quant Struct Act Relat* 1988; 7: 18-25.
10. Klebe G *et al.* Molecular similarity indices in a comparative analysis (CoMSIA) of drug molecules to correlate and predict their biological activity. *J Med Chem* 1994; 37: 4130-4146.
11. Nag SK *et al.* Optimization and structure-activity relationships of a series of potent inhibitors of methicillin-resistant *Staphylococcus aureus* (MRSA) pyruvate kinase as novel antimicrobial agents. *Bioorg Med Chem* 2012; 20: 7069-7082.
12. Wold S, Johansson A, Cochi M. PLS-Partial least squares projection to latent structures. In: *3D-QSAR in drug design: theory, methods and application*, Kubinyi H, ed, ESCOM, Liedin, **1993**; pp. 523-550.
13. Axerio-Cilies P *et al.* Cheminformatics-Driven Discovery of Selective, Nanomolar Inhibitors for Staphylococcal Pyruvate Kinase. *ACS Chem Biol* 2012; 7: 350-359.
14. Schrödinger LLC (2005) Glide, Version 4.0. New York, NY
15. Friesner RA *et al.* Glide: a new approach for rapid, accurate docking and scoring. 1. Method and assessment of docking accuracy. *J Med Chem* 2004; 47: 1739-1749.
16. Richard A *et al.* Extra Precision Glide: Docking and Scoring Incorporating a Model of Hydrophobic Enclosure for Protein-Ligand Complexes. *Med Chem* 2006; 49: 6177-6196.
17. Sybyl version 6.9 (1999) Tripos Associates, St. Louis (MO)
18. Gasteiger J, Marsili M. Iterative partial equalization of orbital electro negativity a rapid access to atomic charges. *Tetrahedron* 1980; 36: 3219-3228.